Title
Retinal tissue engineering using mouse retinal progenitor cells and a novel biodegradable, thin-film poly(e-caprolactone) nanowire scaffold.

Journal
Journal of ocular biology, diseases, and informatics, 1(1)

ISSN
1936-8437

Authors
Redenti, Stephen
Tao, Sarah
Yang, Jing
et al.

Publication Date
2008-03-01

DOI
10.1007/s12177-008-9005-3

j ocul biol dis inform (2008) 1:19–29
DOI 10.1007/s12177-008-9005-3

Retinal tissue engineering using mouse retinal progenitor cells and a novel biodegradable, thin-film poly(e-caprolactone) nanowire scaffold

Stephen Redenti · Sarah Tao · Jing Yang · Ping Gu · Henry Klassen · Sunita Saigal · Tejal Desai · Michael J. Young

Received: 8 February 2008 / Accepted: 4 April 2008 / Published online: 22 May 2008

Abstract Retinal progenitor cells (RPCs) can be combined with nanostructured polymer scaffolds to generate composite grafts in culture. One strategy for repair of diseased retinal tissue involves implantation of composite grafts of this type in the subretinal space. In the present study, mouse retinal progenitor cells (RPCs) were cultured on laminin-coated novel nanowire poly(e-caprolactone)(PCL) scaffolds, and the survival, differentiation, and migration of these cells into the retina of C57bl/6 and rhodospsin −/− mouse retinal explants and transplant recipients were analyzed. RPCs were cultured on smooth PCL and both short (2.5 μm) and long (27 μm) nanowire PCL scaffolds. Scaffolds with adherent mRPCs were then either co-cultured with, or transplanted to, wild-type and rhodopsin −/− mouse retina. Robust RPC proliferation on each type of PCL scaffold was observed. Immunohistochemistry revealed that RPCs cultured on nanowire scaffolds increased expression of mature bipolar and photoreceptor markers. Reverse transcription polymerase chain reaction revealed down-regulation of several early progenitor markers. PCL-delivered RPCs migrated into the retina of both wild-type and rhodopsin knockout mice. The results provide evidence that RPCs proliferate and express mature retinal proteins in response to interactions with nanowire scaffolds. These composite grafts allow for the migration and differentiation of new cells into normal and degenerated retina.

Keywords Tissue engineering · Retina · Stem · Progenitor cells · Biomimetic · Nanotechnology · Polymer · Transplantation

S. Redenti · S. Saigal · M. J. Young (✉)
Ophthalmology, Schepens Eye Research Institute/Harvard Medical School,
20 Staniford Street,
Boston, MA 02114, USA
e-mail: michael.young@schepens.harvard.edu

S. Tao · T. Desai
Physiology, University of California San Francisco,
UCSF MC2520,
Byers Hall Rm203C, 1700 4th Street,
San Francisco, CA 94158-2330, USA

J. Yang · P. Gu · H. Klassen
Department of Ophthalmology, University of California Irvine,
118 Med Surge I,
Orange, CA 92697-4375, USA

Present address:
S. Tao
The Charles Stark Draper Laboratory, Inc.,
555 Technology Square,
Cambridge, MA 02139-3563, USA

Introduction

A number of advances have resulted from recent efforts to repair retinal tissue damaged by disease. Age-related macular degeneration and retinitis pigmentosa are two examples of diseases in which there is loss of photoreceptor cells. While the adult mammalian retina lacks the ability to spontaneously regenerate, a growing body of evidence supports the hypothesis that retinal tissue can be replaced and some degree of functional recovery regained following the delivery of retinal progenitor cells (RPCs) to the subretinal space [1–2]. Subretinally transplanted progenitor cells have the capacity to migrate into the adult retina by following the radially oriented resident glial cells [3]. However, studies using subretinal cell injection lose high

percentages of RPCs due to cell death and efflux during the transplantation process [1, 4]. In recent work, it was demonstrated that the delivery of RPCs on polymer scaffolds results in significantly higher survival of transplanted cells and consequently higher levels of RPC integration [4]. To further enhance RPC survival and direct differentiation, this study implements a novel biodegradable nanostructured poly(e-caprolactone) (PCL) scaffold for cell seeding and subretinal transplantation [5]. The PCL scaffold provides a transient structure for high cell number delivery to localized regions of photoreceptor cell loss.

A novel feature of this PCL scaffold is a topology of vertically oriented nanowires designed to facilitate RPC adhesion and growth [5]. The PCL nanowires are formed by hot melt template synthesis with an average diameter of 150–200 nm and an interwire distance of 20 nm. By varying melt temperature and contact time, nanowire lengths can be specifically tailored. Here, two nanowire lengths were examined: short (2.5 μm) and long (27.5 μm). In the in vitro component of this study, short nanowire (SNW), long nanowire (LNW), and smooth (control) PCL scaffolds were evaluated for their influence on the genetic expression and proliferative capacity of RPCs. Previous studies have shown that polymer scaffold topologies can direct progenitor cell morphology and gene expression [6–8].

A primary objective in this study was to evaluate the proliferative capacity and gene expression of RPCs seeded on PCL composites in vitro. We hypothesized that RPC gene expression could be directed towards mature retinal cell types when in contact with the nanowire surface. Secondly, we studied the migration and differentiation of RPCs delivered on PCL scaffolds into normal and degenerative retinal explant models. Finally, RPC–PCL composites were transplanted into the subretinal space of C57bl/6 and Rho −/− mice for one month. Highly organized and concentrated numbers of RPCs delivered on PCL scaffolds in vivo and we observed the integration, differentiation, and long-term survival of the transplanted cells.

Methods

Mouse progenitor cell isolation and culture

All experiments were performed according to the Schepens Eye Research Institute Animal Care and Use Committee and the ARVO Statement for the Use of Animals in Ophthalmic and Vision Research. Isolation of RPCs was performed as previously described [4]. Briefly, retinas were isolated from postnatal day 1 enhanced green fluorescent protein positive (GFP^+) transgenic mice (C57BL/6 background). Pooled retina were dissociated by mincing and digested with 0.1% type 1 collagenase (Sigma-Aldrich; St. Louis, MO, USA) for 20 min. The liberated RPCs were passed through a 100-mm mesh filter, centrifuged at 850 rpm for 3 min, resuspended in culture medium [Neurobasal (NB); Invitrogen-Gibco, Rockville, MD, USA] containing 2 mM L-glutamine, 100 mg/ml penicillin–streptomycin, 20 ng/ml epidermal growth factor (EGF; Promega, Madison, WI, USA) and neural supplement (B27; Invitrogen-Gibco), and plated into culture wells (Multiwell, Becton Dickinson Labware, Franklin Lakes, NJ, USA). Cells were provided 2 ml of fresh culture medium on alternating days for 2–3 weeks until RPCs were visible as expanding non-adherent spheres. RPC cultures were passaged 1:3 every 7 days.

Polymer fabrication

A polymer casting solution was prepared by dissolving PCL in dichloromethane (4% *w*/*v*) (Sigma-Aldrich). The PCL solution was cast onto a nanoporous anodized aluminum oxide template using a spin coater (Specialty Coating Systems, Indianapolis, IN, USA). The solvent was allowed to evaporate at room temperature. Polymer melts were formed at 130°C while in contact with the nanoporous template. Nanowire length was tuned as a function of melt time. A melt time of 5 min formed nanowires 2.5 μm in length, while a melt time of 60 min formed nanowires 27.5 μm in length. The thin-film scaffold of vertically aligned nanowires was released by etching the template in a dilute sodium hydroxide solution and allowed to air dry at room temperature. Smooth control PCL scaffolds were fabricated on an electrochemically polished silicon wafer using a spin-cast/solvent evaporation method.

Polymer preparation, cell seeding, and culture

PCL nanowire and smooth scaffolds (4×4 mm) were incubated in 70% ethanol for 24 h and rinsed three times with phosphate-buffered saline solution (PBS). PCL scaffolds were placed into single wells of 12-well culture plates and incubated in 50–100 μg/ml mouse laminin (Sigma) in PBS for 12 h to facilitate subsequent adhesion of RPCs in culture. Polymers were then rinsed three times with PBS and transferred to 0.4 μm pore culture well inserts (Falcon) in 12-well plates. Scaffolds were then submerged in 1 ml of NB and incubated for 1 h at 37°C. Cultured GFP^+ RPCs were dissociated into single cell suspensions and 100 μl (4×10^5 cells) seeded onto each laminin-coated PCL membrane. The total volume of each well was brought to 2 ml with additional NB media, and RPCs were allowed to proliferate on the polymers for 7 days.

Scanning electron microscopy

Cell morphology on smooth, SNW, and LNW PCL substrates was examined using scanning electron micros-

copy (SEM) after 1, 3, and 7 days of culture. Before imaging, the cells were fixed and dehydrated. Each sample was rinsed twice in PBS and then soaked in a primary fixative of 3% glutaraldehyde, 0.1 M of sodium cacodylate, and 0.1 M sucrose for 72 h. The surfaces were subjected to two 5-min washes with a buffer containing 0.1 M sodium cacodylate and 0.1 M sucrose. The cells were then dehydrated by replacing the buffer with increasing concentrations of ethanol for 10 min each. The cells were dried by replacing ethanol with hexamethyldisilazane (Polysciences) for 10 min and subsequently air-dried for 30 min. After mounting, the samples were sputter-coated with a 15-nm layer of gold–palladium at a current of 20 mA and a pressure of 0.05 mbar for 45 s. SEM imaging was conducted on a FEI XL30 Sirion scanning electron microscope at 5 kV.

Cell growth and proliferation on PCL

Expansion of GFP^+ RPCs was analyzed on SNW, LNW, and smooth PCL. To establish a standard RPC population curve, total RPC GFP^+ signals were detected in populations from 1×10^3–1.5×10^5 in 96-well plates (n=4) using a Tecan, Genios microplate reader. A 1.0×1.0-mm piece of each PCL subtype was then seeded with RPCs and cultured for 7 days. Total GFP emissions from RPCs on each polymer type were taken at days 1, 3, and 7 under identical conditions. The RPC–polymer signals and standard population curve signals were then correlated to establish polymer cell density. The composites were also imaged at 10× magnification at days 1, 3, and 7. After the initial seeding of cells a Spot ISA-CE camera (Diagnostic Instruments, Sterling Heights, CA, USA) attached to a Nikon Eclipse TE800 microscope was used to visualize cell proliferation across each PCL subtype surface.

Immunohistochemistry

After culturing RPCs for 7 days, RPC–polymer composites were rinsed three times with PBS (warmed to 37°C) and fixed in 4% paraformaldehyde for 1 h, cryoprotected first in 10% sucrose for 12 h and then in 30% sucrose for 12 h. Cryoprotected composites were frozen in optimal cutting temperature compound (Sakura Finetek, Torrence, CA) at −20°C and cut into 20-μm sections using a Minotome Plus (Triangle Biomedical Sciences, Durham, NC, USA). All samples were rinsed 3×10 min in PBS and then blocked and permeabilized in PBS containing 10% goat serum, 1% bovine serum albumin, and 0.1% Triton-X for 2 h. Samples were incubated with primary antibodies using a dilution of 1:200 for CRX (Santa Cruz), 1:500 for PKC (Sigma), 1:400 for Nestin (BD Biosciences), 1:100 for Ki67 (Sigma), 1:200 for 4D2 (a gift from Prof. Robert Molday, University of British Columbia, Canada), 1:200 for GFAP (Zymed), 1:100 for Recoverin (Abcam), and 1:1,000 for NF-200 (Sigma) in blocking buffer for 12 h at 4°C. Samples were then rinsed 3×10 min in PBS and incubated with a Cy3-labeled secondary antibody 1:800 (Zymed) and Toto-3 (Molecular Probes) nuclear stain for 2 h at room temperature. Finally, samples were rinsed 3×10 min in PBS and sealed in mounting medium (Vector Laboratories) for imaging using a Leica TCS SP2 confocal microscope.

Reverse transcription–polymerase chain reaction

Total RNA was extracted from cultured cells using the RNeasy mini kit according to the manufacturer's instructions (Qiagen, CA, USA) followed by in column treatment with DNase I (Qiagen). Reverse transcription was performed with Omniscriptase reverse transcriptase (Qiagen) and random primers (Sigma). Amplification of β-actin served as the internal control. The primers for reverse transcription–polymerase chain reaction (RT-PCR) are shown in Table 1. Amplification conditions were 40 s/94°C, 40 s/55°C, 1 min/72°C for 35 cycles. Table 1. List of primers for RT-PCR.

Table 1 List of primers for RT-PCR

Gene	Primer sequence (5′-3′)	Product size (bp)
Nestin	F: AACTGGCACACCTCAAGATGT	235
	R: TCAAGGGTATTAGGCAAGGGG	
Sox2	F: CACAACTCGGAGATCAGCAA	190
	R: CTCCGGGAAGCGTGTACTTA	
Pax6	F: AGTGAATGGGCGGAGTTATG	132
	R: ACTTGGACGGGAACTGACAC	
Hes1	F: CCCACCTCTCTCTTCTGACG	185
	R: AGGCGCAATCCAATATGAAC	
Hes5	F: CACCGGGGGTTCTATGATATT	180
	R: CAGGCTGAGTGCTTTCCTATG	
Ki-67	F: CAGTACTCGGAATGCAGCAA	170
	R: CAGTCTTCAGGGGCTCTGTC	
β-tubulin III	F: CGAGACCTACTGCATCGACA	152
	R: CATTGAGCTGACCAGGGAAT	
Dex	F: ATGCAGTTGTCCCTCCATTC	182
	R: ATGCCACCAAGTTGTCATCA	
Recoverin	F: ATGGGGAATAGCAAGAGCGG	179
	R: GAGTCCGGGAAAAACTTGGAAATA	
Rhodopsin	F: TCACCACCACCCTVTACACA	216
	R: TGATCCAGGTGAAGACCACA	
GFAP	F: AGAAAACCGCATCACCATTC	184
	R: TCACATCACCACGTCCTTGT	
β-actin	F: AGCCATGTACGTAGCCATCC	228
	R: CTCTCAGCTGTGGTGGTGAA	

Retinal explant culture

C57bl/6 (n=3) and rhodopsin knockout (Rho−/−; n=3) mice were euthanized and their eyes enucleated immediately and placed in ice-cold PBS. The anterior portion of each eye was removed along with vitreous. Four radial cuts were made into the posterior eyecup and each quadrant flattened sclera side down. The flattened eyecup was then cut into four separate pieces (~2.0×2.0 mm) and transferred to a 0.4-μm culture well insert, ganglion side down, and sclera removed. Culture well inserts containing retina were placed into six-well culture plates. Two milliliters of NB was added to each culture well. Onto each retinal explant, a 7 day cultured RPC–PCL (2.0×1.0 mm) composite was placed with wire surface toward retina. Three SNW, LNW, and smooth RPC seeded PCL constructs (n=18) were added to both C57bl/6 and Rho−/− explants and co-cultured for 1 week in NB at 37°C.

Subretinal transplantation surgery

Transplantation surgeries were performed as previously described [4]. Briefly, SNW and LNW PCL scaffolds with adherent RPCs were cut into 1.0×0.5-mm sections using a sterile scalpel in preparation for transplantation. Mice were placed under general anesthesia with an intraperitoneal injection of ketamine (5 mg/kg) and xylazine (10 mg/kg) and the pupil dilated with 1% tropicamide, topically applied. Proparacaine (Akorn), a topical anesthetic, was applied to the eye. Mice were placed on a warm heating blanket for surgery. Silk suture (8–0) was used to retract the eyelid, and the globe was stabilized for surgery using a single 11–0 conjuctival suture. An incision (0.5–1.0 mm) was made in the lateral posterior sclera using a Sharpoint 5.0-mm blade scalpel (Fine Science Tools, Reading, PA, USA). PCL-RPC composites were inserted through the sclerotomy into the subretinal space using no. 5 Dumont forceps (Fine Science Tools). A single eye from each C57BL/6 wild-type mouse (n=10) and Rho −/− mouse (n=10) received a subretinal transplant. The scleral incision was closed with an 11–0 nylon suture and all other sutures were removed. Additional proparacain was applied and mice were allowed to recover. Transplants remained in the subretinal space for 1 month.

Histologic preparation of transplanted tissue

C57BL/6 mice that received composite grafts were killed after 4 weeks. Engrafted eyes were enucleated, immersion fixed in 4% paraformaldehyde, rinsed three times in PBS, and cryoprotected in 10% then 30% sucrose for 12 h each at 4°C. Eyes were then placed in a cryomold containing optimum cutting temperature compound (ProSciTech) and then frozen on dry ice and cryo-sectioned at 20 μm.

Results

Polymer preparation, cell seeding, and culture

RPC survival and proliferation were similar when cultured on each type of PCL scaffold studied (Fig. 1). After seeding 4×10^5 cells into culture wells containing 1.0×1.0 mm PCL scaffolds, a similar number of cells had adhered to each topology type as revealed by averaged GFP^+ fluorescence intensities (Fig. 1a). Cell numbers increased steadily for the remaining 7 days in culture. At days 1, 3, and 7, the averaged (n=3) number of cells were SNW: 10677(±6229),

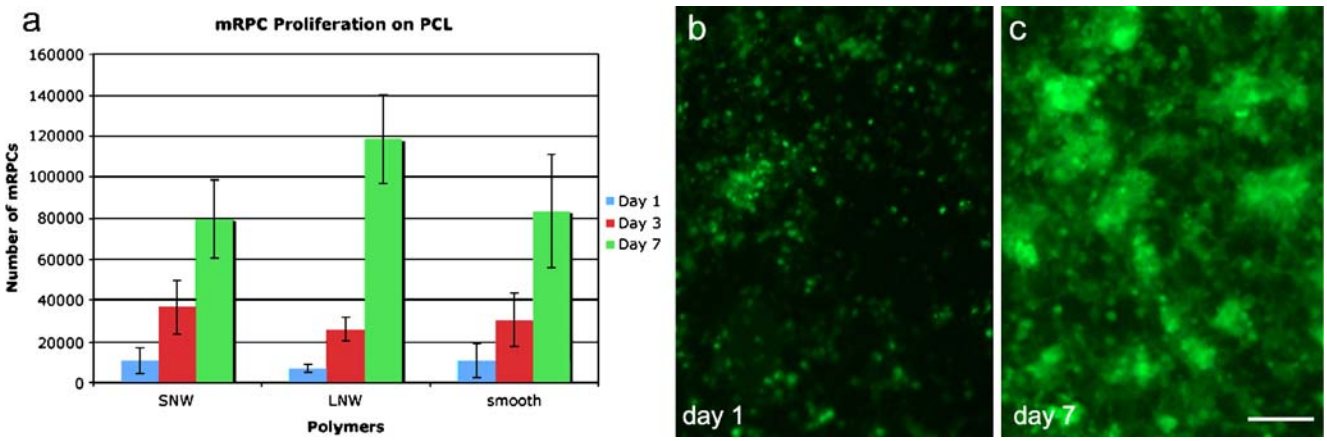

Fig. 1 GFP^+ RPC Growth on Poly(e-caprolactone). PCL is template-synthesized to form short (~2.5 μm) fiber length (*SNW*), long (~27 μm) fiber length (*LNW*) and smooth control scaffolds. **a** Proliferation of GFP^+ mRPCs cultured on short, long, and smooth PCL scaffolds evaluated over 7 days. The average numbers of adherent mRPCs at days 1, 3, and 7 on SNW were 10677, 36478, 79308, LNW were 6799, 26044, 118395, and smooth were 10723, 26037, 83205, respectively. **b**, **c** Fluorescent micrograph of GFP^+ mRPCs on LNW scaffolds at days 1 and 7 after initial 24 h adherence periods, respectively. Error bar: SEM; scale, 100 μm

36478(±12753), 79308(±19057), LNW: 6799(±1867), 26044(±5681), 118395(±21865), and smooth: 10723 (±8523), 26037(±12722), 83205(±27582), respectively. RPC densities at day 1 increased through day 7 and can be seen in Fig. 1b and c, respectively.

Scanning electron microscopy of mRPC-seeded scaffolds

RPCs cultured at low densities for SEM imaging on nanowire PCL exhibited apparent polymer topology attachment patterns and/or morphologic changes at 3 and 7 days (Fig. 2). The most pronounced morphologic changes occurred in RPCs cultured on SNW PCL at days 3 and 7 (Fig. 2a and b). On SNW, individual RPCs adhered to clustered tips of 2.5 μm nanowires and spread fan-like processes (~20 nm) out to neighboring cells, creating apparent cell-to-cell contacts. RPCs cultured on LNW PCL formed small clusters on the underside of wave-like aggregates of the 27.5-μm nanowires and maintained their spheroid shape at days 3 and 7 (Fig. 2c and d). RPCs seeded onto smooth PCL adhered at random intervals to each surface and showed no distinctive morphologic changes at either day 3 or 7 and exhibited no alignment with specific surface regions (Fig. 2e and f).

Immunohistochemistry

Immunohistochemical analysis of RPCs cultured on PCL revealed that scaffold topology influenced protein expression levels (Fig. 3). The markers used to evaluate RPC differentiation included the early photoreceptor marker CRX, the bipolar cell marker PKC, the neural progenitor marker nestin, the active cell cycle marker Ki67, the mature photoreceptor marker 4D2, the glial cell marker GFAP, the photoreceptor marker recoverin, and the neural filament maker nf-200. On each subtype of PCL polymer, RPCs consistently labeled positively for nestin and nf-200, indicating the presence of undifferentiated cell populations. Mouse RPCs cultured on SNW and LNW nanowire scaffolds demonstrated evidence of differentiation including increased expression of PKC and recoverin. Smooth PCL produced no detectable changes in RPC expression of

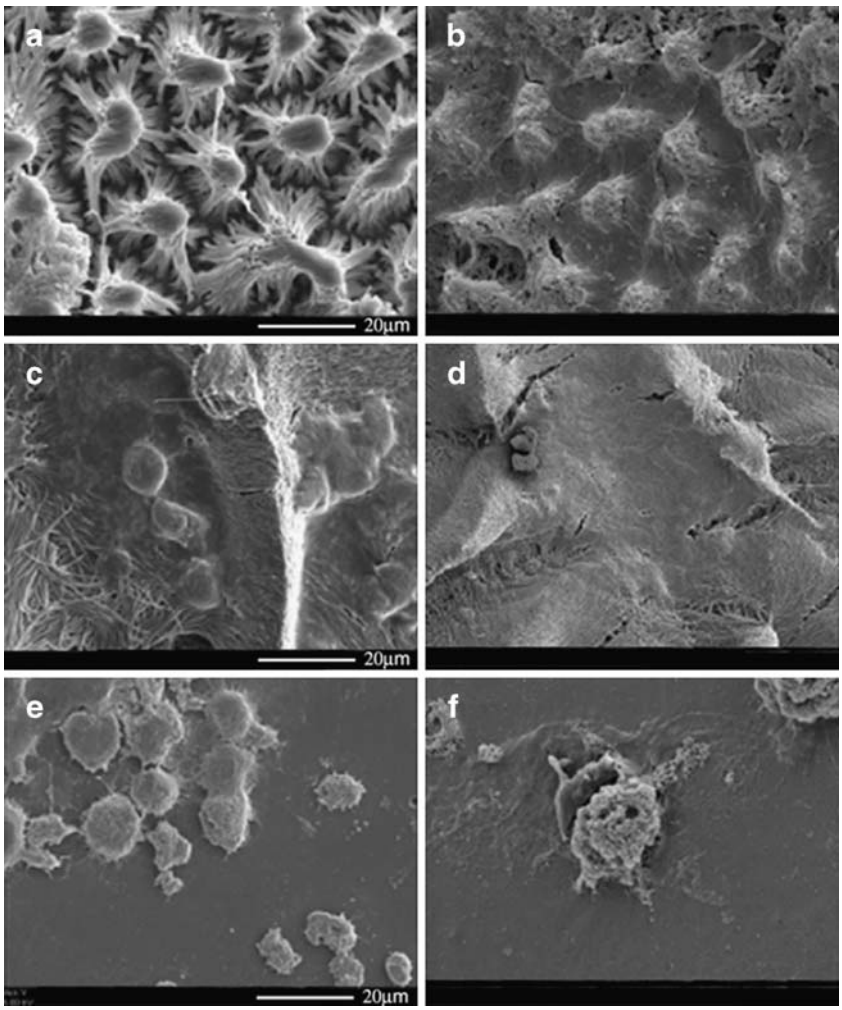

Fig. 2 Scanning electron microscopy of RPCs Cultured on SNW, LNW, and smooth PCL scaffolds. RPCs, with 10–20 μm diameter, were seeded and allowed to proliferate for 7 days. **a**, **b** RPCs develop on the upper edge of aggregated short nanowires extending lamelapodia-like structures towards adjacent cells on days 3 and 7, respectively. **c d** RPCs seeded and attached to the vertical edges formed by long nanowires on days 3 and 7. RPCs on LNW retain a typical spheroid shape. **e f** Smooth PCL allows for RPCs to adhere randomly without topographic cues at days 3 and 7

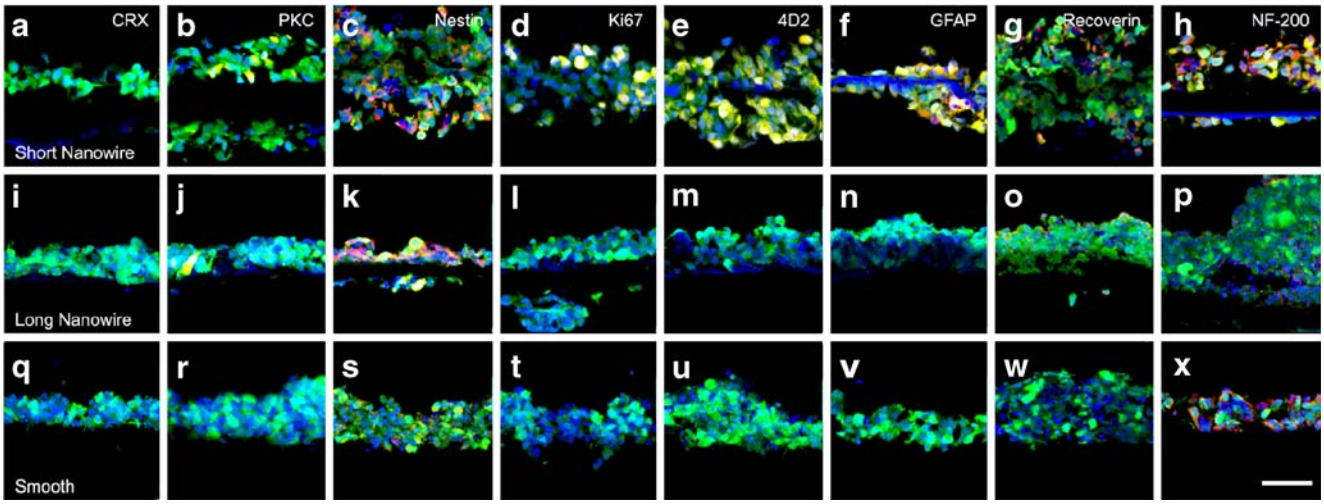

Fig. 3 Characterization of RPCs cultured on PCL scaffolds for 7 days. **a**–**h**, **i**–**p**, **q**–**x** Short nanowire, long nanowire, and smooth RPC-seeded PCL scaffolds, respectively. **a**, **i**, **q** CRX did not show expression. **b**, **j**, **r** PKC showed expression only on SNW and LNW. **c**, **k**, **s** While Nestin was expressed on SNW, LNW, and smooth, **d**, **l**, **t** Ki67 and **e**, **m**, **u** 4D2 were only expressed on SNW. The glial cell marker (**f**, **n**, **v**) GFAP was expressed on SNW and smooth PCL. **g**, **o**, **w** Recoverin was only expressed on LNW and SNW. **h**, **p**, **x** nf-200 showed expression on each scaffold. Each image is overlaid with *green* = GFP RPCs, *red* = cy3-bound primary marker, and *blue* = nuclei labeled with Toto 3. Scale, 50 μm

mature retinal neural markers. Interestingly, SNW topology induced increases in the rod photoreceptor protein rhodopsin as well as recoverin and PKC.

Reverse transcription–polymerase chain reaction

Analysis of RNA synthesis in RPCs using RT-PCR revealed marked down-regulation of Pax6, Hes1, B3-tubulin, DCX and partial down-regulation of nestin and Sox2 (Fig. 4). GFAP was up-regulated. Decreases in the expression levels of Pax6, Hes1, nestin, and Sox2 suggest that the immature RPCs had begun undergoing differentiation toward more mature states while co-cultured on the polymer scaffolds.

Migration and differentiation of RPCs in retinal explants

At 1 week, RPC-PCL composites of each topology type cultured on either C57bl/6 or Rho−/− retinal explants allowed for RPC migration into each retinal layer and expression of location-appropriate, fate-specific markers (Fig. 5). Both C57bl/6 and Rho−/− mouse retinal explants proved permissive environments for the migration of progenitor cells to specific retinal layers. Both SNW and LNW RPC composites resulted in high levels of migration into the inner nuclear and ganglion cell layers (INL, GCL) of the Rho−/− explants. Smooth PCL RPC composites did not provide for integration into the Rho−/− model. Widespread integration of RPCs into C57bl/6 retinal lamina was seen (Fig. 5a–c). The soma of integrated RPCs aligned with host nuclear layers, from which they extended processes toward and into each plexiform layer. RPC-

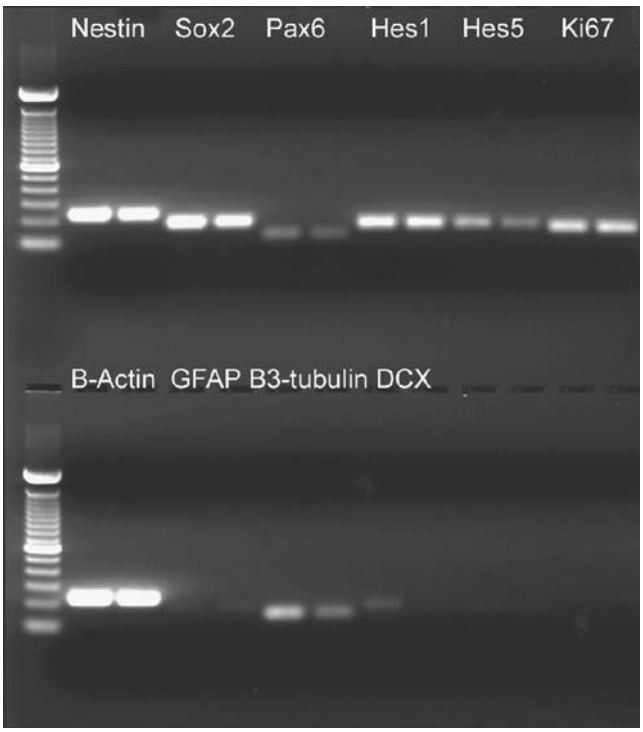

Fig. 4 RT-PCR of RPCs on PCL. RPC expression under standard culture conditions and at day 7 on SNW. Each gene of interest is tested pairwise: The *first lane* is baseline expression, the *second* is day 7 on PCL. Genes that are clearly down-regulated after 7 days of culture on PCL were Pax6, Hes5, B3-tubulin, DCX. Partially down-regulated genes included Nestin and Sox2. The primary up-regulated gene was GFAP

SNW and LNW composites cultured on explants developed into profiles similar to glial, bipolar, and rod phenotypes. The migration and differentiation of RPCs was not significantly different between SNW and LNW explants. Three dimensional views of RPC integration from SNW and LNW composites into 20-μm-thick explants reconstructed from 1-μm confocal scans can be seen in Fig. 6a–d, respectively. The expression of PKC and recoverin were seen in RPCs that migrated into the outer and inner plexiform (OPL, IPL) layers, respectively (Fig. 6b and d).

RPC migration and differentiation following subretinal transplantation

Based on lower RPC proliferation and migration into explants, smooth PCL was not transplanted in vivo. After 1 month in the subretinal space of C57bl/6 and Rho−/− mice, RPCs grafted on LNW and SNW scaffolds had migrated into specific retinal laminae, extended processes and differentiated morphologically (Figs. 7 and 8). In normal C57bl/6 mice, many RPCs migrated to the INL/IPL region and adopted a morphology similar to glial or amacrine cells with processes, extending 10–50 μm. RPCs that migrated to the IPL showed expression of GFAP (Fig. 7a and b). Projections from RPC soma integrated into the IPL, extended through the IPL, and occasionally reached into both the IPL and GCL layers. RPCs which migrated into the outer nuclear and outer plexiform layers (Fig. 7c and d; ONL, OPL) extended shorter (~5–10 μm) processes remaining in the ONL or extending into the OPL. RPCs that migrated into the outer retina appeared to connect in regions with cells expressing either PKC or recoverin, respectively (Fig. 7c and d). A high number of RPCs were seen to have migrated into host retinal tissue directly adjacent to the site of transplantation. In Rho−/− recipients, RPCs migrated into the degenerated ONL and into the remaining INL and GCL (Fig. 8a). A number of RPCs that had migrated into the Rho−/− retina ONL and INL developed an apparent cell polarity with early photoreceptor-like morphology, while mRPCs adjacent to the IPL expressed GFAP (Fig. 8b). Unique to the Rho−/− recipients, small diameter (~10 μm) RPCs migrated into the ONL and expressed recoverin (Fig. 8c). The area of host retinal integration was approximately 0.3×0.8 μm, similar to the transplant size. We observed highly localized delivery of RPCs incorporated into the host retinal laminae across the area of the transplant.

Discussion

In this study, we show that RPCs can be co-cultured with PCL nanowire substrates and that these scaffolds are biologically compatible with RPCs, as evidenced by cell adhesion and

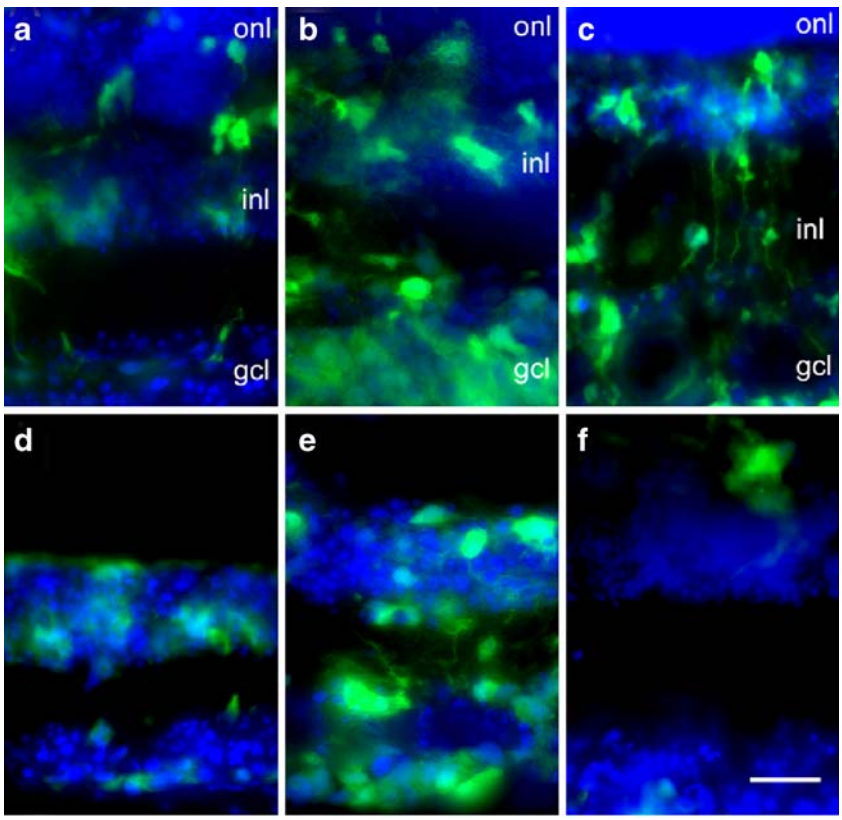

Fig. 5 PCL scaffold delivery of GFP^+ RPCs to C57bl/6 and Rho −/− mouse retinal explants. **a**–**c** Migration of GFP mRPCs from SNW, LNW, and smooth PCL scaffolds, respectively, into C57bl/6 retinal explants at day 7. Scaffolds were seeded with ~2.5×10^5 day P0 GFP^+ mRPCs and allowed to proliferate in vitro for 7 days. Cells migrated into each retinal layer. **d**, **e** mRPC migration from SNW and LNW PCL into each cellular (nuclear) layer of the Rho −/− retinal explants. Note that the outer nuclear layer is absent from the 8- to 10-week Rho −/− retina due to degeneration. **f** Few mRPCs delivered on smooth PCL appeared to enter the Rho −/− retina. Scale, 100 μm

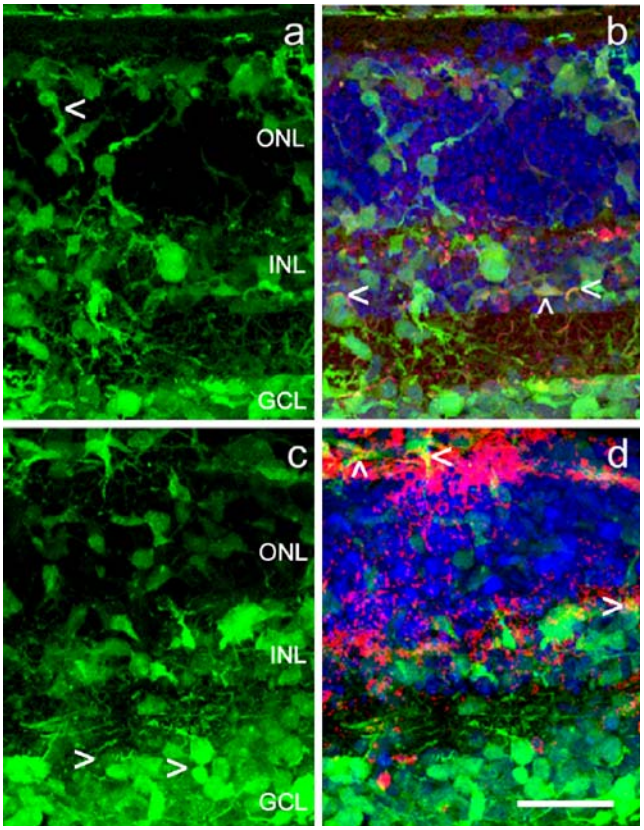

Fig. 6 Differentiation and 3D reconstruction of GFP$^+$ RPCs delivered to a C57bl/6 retinal explant via nanowire PCL scaffolds. **a**, **b** 20-μm thick explant section reconstructed from successive 1-μm confocal scans showing high levels of RPC integration from cells delivered by SNW. Also, in the ONL, a transplanted RPC exhibits a potential immature photoreceptor morphology (*arrow*). **b** PKC (*red*) double labeling (*arrows*) of RPC soma and processes from image **a** incorporated into the INL of host retina. **c**, **d** High numbers of RPCs migrated into the GCL (*arrows*) from LNW. **d** Recoverin (*red*) labeled RPCs (*arrows*) in the ONL region of host explant. Scale: 100 μm

sustained proliferation. This work complements and builds on earlier studies which analyzed the biocompatibility of micro-patterned polymer substrates both in vitro and in vivo [4, 7, 9]. To avoid physical distortion and metabolic impairment of the outer retina, implantation in the subretinal space puts a premium on the thinness of the scaffold used. The nanowire scaffolds presented here represent the thinnest and most intricately patterned polymer substrates that have been used for RPC subretinal transplantation to date.

The basement PCL sheet from which both short and long nanowires project is, on average, 6.00±0.70 μm thick. The thin-film structure of nanowire PCL offers two significant advantages for subretinal transplantation. Firstly, RPC-seeded PCL scaffolds can be placed into the subretinal space with minimal disturbance of surrounding tissue. Secondly, PCL is highly permeable, allowing for the passage of physiologically significant molecules and has a predictable degradation rate. After 7 weeks in saline, nanowire features are completely degraded [5]. The biodegradation of PCL occurs gradually from its surfaces and shows no pathologic increases in local acidity as seen in the bulk degradation of polymers composed of higher molecular weight ie: PGLA [10]. The nanoscale architecture and degradation rate of PCL nanowire scaffolds are well suited for subretinal RPC delivery.

Polymer substrates for tissue engineering with either nanowire or micro-patterned porous three-dimensional structures have been shown to enhance progenitor cell adhesion [7, 9]. In a recent study, it was demonstrated that poly(methyl methacrylate) (PMMA) scaffolds micro-machined to contain through pores provided greater RPC adhesion during transplantation than a non-structured PMMA control [9]. For the purpose of RPC culture and eventual delivery of RPCs into the subretinal space, an optimal polymer scaffold should provide either surface or internal cavities to protect cell-to-polymer contacts from mechanical and shearing forces. The surface patterning of PCL nanowire scaffolds provide niches for secure and organized cell adhesion.

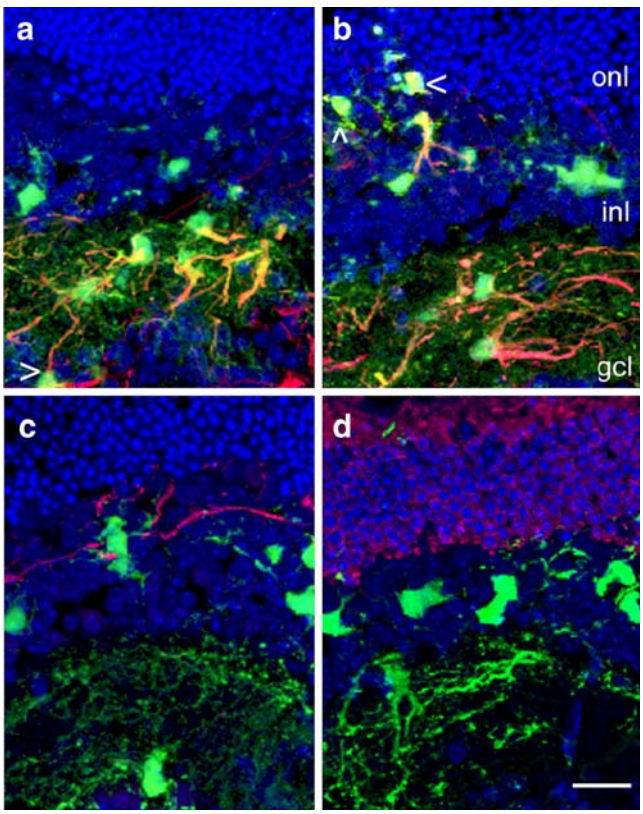

Fig. 7 GFP$^+$ RPC migration, integration, and differentiation in host retina 30 days following subretinal transplantation. **a**, **b** Transplanted GFP$^+$ RPC soma migrate into each retinal layer and co-label for GFAP (*red*). **a** RPC migrated into GCL extend visible processes into IPL (*arrow*). **b** Smaller RPCs migrated into ONL and appear to have short processes in the OPL region (*arrows*). **c**, **d** Transplanted RPCs integrate into the OPL region of host retina expressing normal levels of NF-200 (**c**) and recoverin (**d**)

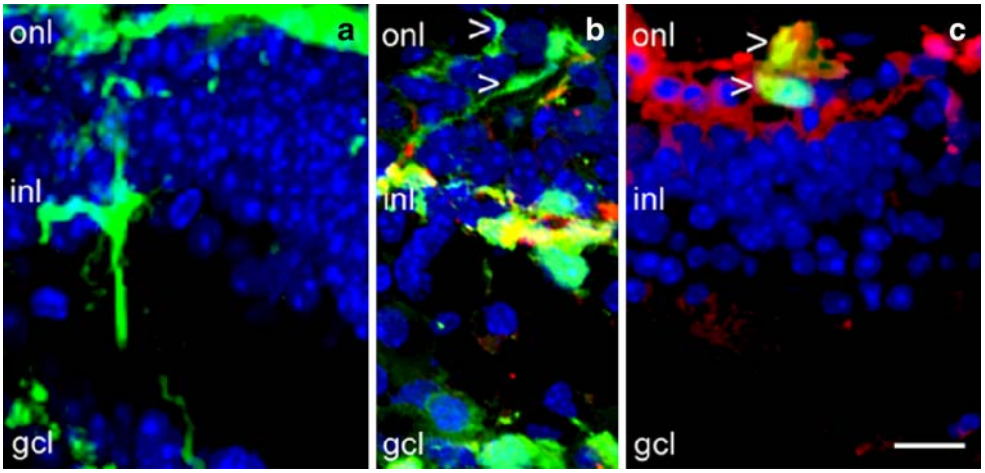

Fig. 8 GFP$^+$ RPC migration, integration and differentiation in Rho−/− retina 30 days following subretinal transplantation. **a** Transplanted mRPCs migrate into the degenerated Rho−/− ONL and into the preserved INL and GCL. **b** mRPCs migrated into ONL and INL exhibit an early photoreceptor-like morphology (*arrows*), while RPCs adjacent to the IPL express GFAP. **c** Small RPCs migrated into ONL express GFP and label positively for recoverin (*red*; *arrows*)

Combining cells with polymer substrates to engineer implants directed at repairing retinal tissue requires attention to the interacting properties of the particular cell type and the chosen polymer. In the present study, it was important to consider the relationship between the response properties of the selected RPC population and the microenvironment of the PCL nanowire scaffolds, particularly with respect to how this might influence retinal cell fates. The RPCs used in this study were isolated from GFP$^+$ C57BL/6 mice at post-natal day 0 (P0), a developmental time shown to produce primarily rod, bipolar, and Mueller cells [11–13]. The transient expression of Notch and yan receptors by P0 RPCs provide examples of known pathways capable of influencing cell fate in response to exogenous signaling. In a further example, in the presence of ciliary neurotrophic factor (CNTF), which is produced by the developing retina, higher numbers of P0 RPCs can be driven to express opsin [12]. After time in culture, P0 RPCs not expressing opsin and exposed to CNTF tend to differentiate toward a bipolar cell fate [14]. Under the proliferation conditions used in this study, RPCs were incubated in elevated levels (20 ng/ml) of EGF to maintain mitogenic activity. According to one report, P0 RPCs transiently express the EGF receptor and proliferate in response to EGF via a Notch signaling pathway [15]. It has also been reported that exposure to EGF has the potential to override intrinsic fate cues of late progenitors and drive differentiation towards a glial fate [15–16]. Our earlier study demonstrated that PLGA scaffolds tend to sequester EGF from the surrounding medium, and the PCL material used in the current study might potentially behave in a similar manner. In this way, GFAP expression by RPCs on SNW in vitro might result from availability of EGF and hence the influence of EGF signaling on cell competence. Another possibility is that treatment of scaffolds with the substrate laminin, used to promote cellular adherence for transplantation, might also have contributed to the observed changes in cellular behavior.

The morphologic changes of RPCs that occurred in response to SNW scaffold architecture involved the anchoring of cell soma to aggregated nanowire tips with extension of lamellipodia-like structures toward adjacent cells. The RPCs made apparent contacts with one another forming uniform monolayers across aggregated nanowire bundles. This type of cell morphology across a polymer surface has been referred to as an “adhesion plaque” and serves to strengthen cell-to-substratum attachment [17]. In addition to geometric constraints conferred by the fine structure of the nanowire scaffolds, the morphology of co-cultured RPCs is likely influenced by changes in cellular phenotype occurring under these circumstances, as discussed in previous studies [7, 18]. Taken together, the gene expression patterns and substrate-directed morphologies indicate a trend toward more mature phenotypes for RPCs cultured on laminin-treated PCL nanowire substrates.

The characterization of cycling uncommitted multipotent RPCs is challenged by the tendency of these cells to express a range of different neural and glial fate-related transcripts [19]. Individual multipotent RPCs of similar lineage exhibit transient changes in molecular heterogeneity at different time points. After terminal mitosis, non-fate specific markers are down-regulated, while selected fate markers are more strongly expressed. Even after RPCs have exited the mitotic cycle, they retain a level of plasticity and can change expression patterns and redirect fate [20]. In this study, mitogenic subpopulations of RPCs interacting with PCL nanowires could be seen to up-regulate fate-specific markers. Nevertheless, these results indicate a trend toward a differentiated state rather than clear evidence of terminal differentiation. The nanowire surface appears to be capable of at least partially modifying the growth kinetics, morphology, and expression patterns of adhering progenitor cells.

Co-culture of RPC-containing polymers with retinal explants resulted in migration of the progenitor cells into

each retinal layer. Of the markers evaluated, the transplanted cells reacted for recoverin and PKC expression. The morphology of the migrated cells resembled glial and neural subtypes appropriate to their region of laminar integration. The in vivo subretinally transplanted RPCs also integrated into each lamina with a preference for IPL and GCL layers. The majority of cells labeled for GFAP expression. This finding may be the result of the developmental potential of the selected RPC population for differentiation towards a glial fate and/or partially influenced by EGF exposure as discussed above [15, 21]

In terms of transplantation, based on the number (~100,000) of RPCs attached to 1.0×1.0-mm pieces of SNW and LNW at day 7, we can predict that approximately 50,000 RPCs were delivered on each 0.5×1.0-mm graft that was transplanted. This level of cell delivery was sufficient to achieve direct migration and integration of RPCs from the scaffold into regions of the host retina adjacent to the transplantation site. As this technique evolves, delivering predetermined numbers of RPCs to a specific region of the retina damaged by disease or injury may become a realistic approach to retinal tissue repair [4].

Summary and future directions

The use of polymer scaffolds holds great potential as a means to increase donor cell survival during transplantation of stem cells to the retina. To further refine fate selection for the directed replacement of specific retinal cell types, future work might investigate a range of cell types and exogenous factors. It has also been suggested that the delivery of post-mitotic cells may facilitate differentiation into a selected terminal fate [2, 22]. Additionally, PCL nanowire scaffolds can be fabricated to release proteins shown to direct RPCs towards a photoreceptor fate and promote cell survival. The current work demonstrates the ability of PCL nanowire scaffolds to influence RPC gene expression levels. The PCL scaffold allows RPCs to proliferate and form a cell dense ultra-thin composite graft for subretinal transplantation. The organized PCL–RPC composite allows for controlled and precisely localizable delivery of cells for the potential replacement and restoration of retinal tissue destroyed by disease or trauma.

Acknowledgments We thank Dr. Lynne Chang for assistance with proliferation analysis. Financial support was provided by the Richard and Gail Siegal Gift Fund, the Foundation Fighting Blindness, the Department of Defense, and a grant from the Lincy Foundation and Discovery Eye Foundation (H.K., M.J.Y.). S.R. was supported in part through Harvard Medical School, Molecular Bases of Eye Diseases, National Eye Institute Award T32 EY07145-06.

References

1. Klassen HJ, Ng TF, Kurimoto Y, Kirov I, Shatos M, Coffey P, et al. Multipotent retinal progenitors express developmental markers, differentiate into retinal neurons, and preserve light-mediated behavior. Invest Ophthalmol Vis Sci. 2004;45 11:4167–73 (Nov).
2. MacLaren RE, Pearson RA, MacNeil A, Douglas RH, Salt TE, Akimoto M, et al. Retinal repair by transplantation of photoreceptor precursors. Nature. 2006;444 7116:203–7 (Nov 9).
3. Wojciechowski AB, Englund U, Lundberg C, Warfvinge K. Survival and long distance migration of brain-derived precursor cells transplanted to adult rat retina. Stem Cells. 2004;22 1:27–8.
4. Tomita M, Lavik E, Klassen H, Zahir T, Langer R, Young MJ. Biodegradable polymer composite grafts promote the survival and differentiation of retinal progenitor cells. Stem Cells. 2005;23 10:1579–88 (Nov–Dec).
5. Tao SL, Desai TA. Aligned arrays of biodegradable poly(epsilon-caprolactone) nanowires and nanofibers by template synthesis. Nano Lett. 2007;7 6:695–701 (Jun).
6. Recknor JB, Sakaguchi DS, Mallapragada SK. Growth and differentiation of astrocytes and neural progenitor cells on micropatterned polymer films. Ann N Y Acad Sci. 2005;1049:24–7 (May).
7. Recknor JB, Sakaguchi DS, Mallapragada SK. Directed growth and selective differentiation of neural progenitor cells on micropatterned polymer substrates. Biomaterials. 2006;27 22:4098–108 (Aug).
8. Miller C, Jeftinija S, Mallapragada S. Synergistic effects of physical and chemical guidance cues on neurite alignment and outgrowth on biodegradable polymer substrates. Tissue Eng. 2002;8 3:367–78 (Jul).
9. Tao S, Young C, Redenti S, Zhang Y, Klassen H, Desai T, et al. Survival, migration and differentiation of retinal progenitor cells transplanted on micro-machined poly(methyl methacrylate) scaffolds to the subretinal space. Lab Chip. 2007;7 6:695–701 (Jun).
10. Grayson AC, Voskerician G, Lynn A, Anderson JM, Cima MJ, Langer R. Differential degradation rates in vivo and in vitro of biocompatible poly(lactic acid) and poly(glycolic acid) homo- and co-polymers for a polymeric drug-delivery microchip. J Biomater Sci Polym Ed. 2004;15 10:1281–304.
11. Rapaport DH, Wong LL, Wood ED, Yasumura D, LaVail MM. Timing and topography of cell genesis in the rat retina. J Comp Neurol. 2004;474 2:304–24 (Jun 21).
12. Cepko CL, Austin CP, Yang X, Alexiades M, Ezzeddine D. Cell fate determination in the vertebrate retina. Proc Natl Acad Sci USA. 1996;93 2:589–95 (Jan 23).
13. Livesey FJ, Cepko CL. Vertebrate neural cell-fate determination: lessons from the retina. Nat Rev Neurosci. 2001;2 2:109–18 (review, Feb).
14. Zahir T, Klassen H, Young MJ. Effects of ciliary neurotrophic factor on differentiation of late retinal progenitor cells. Stem Cells. 2005;23 3:424–32 (Mar).
15. James J, Das AV, Rahnenfuhrer J, Ahmad I. Cellular and molecular characterization of early and late retinal stem cells/progenitors: differential regulation of proliferation and context dependent role of Notch signaling. J Neurobiol. 2004;61 3:359–76.
16. Irvin DK, Dhaka A, Hicks C, Weinmaster G, Kornblum HI. Extrinsic and intrinsic factors governing cell fate in cortical progenitor cultures. Dev Neurosci. 2003;25 2–4:162–72 (Mar–Aug).
17. Lu L, Yaszemski MJ, Mikos AG. Retinal pigment epithelium engineering using synthetic biodegradable polymers. Biomaterials. 2001;22 24:3345–55 (review, Dec).
18. Lavik EB, Klassen H, Warfvinge K, Langer R, Young MJ. Fabrication of degradable polymer scaffolds to direct the

integration and differentiation of retinal progenitors. Biomaterials. 2005;26 16:3187–96 (Jun).
19. Trimarchi JM, Stadler MB, Roska B, Billings N, Sun B, Bartch B, et al. Molecular heterogeneity of developing retinal ganglion and amacrine cells revealed through single cell gene expression profiling. J Comp Neurol. 2007;502 6:1047–65 (Jun 20).
20. Belliveau MJ, Young TL, Cepko CL. Late retinal progenitor cells show intrinsic limitations in the production of cell types and the kinetics of opsin synthesis. J Neurosci. 2000;20 6:2247–54 (Mar 15).
21. Klassen H, Sakaguchi DS, Young MJ. Stem cells and retinal repair. Prog Retin Eye Res. 2004;23 2:149–81 (Mar).
22. Canola K, Angenieux B, Tekaya M, Quiambao A, Naash MI, Munier FL, et al. Retinal stem cells transplanted into models of late stages of retinitis pigmentosa preferentially adopt a glial or a retinal ganglion cell fate. Invest Ophthalmol Vis Sci. 2007;48 1:446–54 (Jan).